Progress In Electromagnetics Research Letters, Vol. 72, 119–126, 2018

Reconfigurable Microstrip Antennas Conformal to Cylindrical Surface

Prasanna K. Singh* and Jasmine Saini

Abstract—Conformability helps microstrip antenna to mount on any geometry platform and can also be used for multiple frequency systems without any complexity. The designing of a frequency reconfigurable antenna conformal to cylindrical surface using the combination of metamaterial (MTM) and substrate integrated waveguide (SIW) is proposed. The single and dual antenna models resonate at various frequencies of C-band by means of changing the cylindrical curvature. The results also show a considerable improvement in bandwidth and gain for dual antennas as compared to the single antenna. The antenna parameters are simulated on HFSS tool, and validation process is done by experimental setup.

1. INTRODUCTION

In the era of communication modernisation, microstrip antenna plays a deciding role due to its multitasking potentials and finds new opportunities in many applications. In continuation, active research works are reported by many agencies in the area of non-planar surfaces [1–6]. The recent developments in MTM and SIW in the microstrip antenna have received increased interest and are utilized as an integrated part of cylindrical surface/device [7–11]. Here, a patch antenna model made up of MTM with SIW is mounted on varying cylindrical geometry with superstrate. The variation in frequency is observed due to dielectric bending of substrate and superstrate, which affects the permittivity and thus acts as a frequency reconfigurable antenna. With the increase in bending, the frequency moves to higher side of the band and vice-versa. This hybrid antenna is also useful in achieving the enhanced gain and wide bandwidth by properly utilizing combination of MTM and SIW properties as compared to a simple antenna [12–15]. The antenna model includes an MTM superstrate placed at nearly a quarter wavelength from radiator for the resonance condition. Furthermore, this paper analyses the effect of varying curvature on the antenna performances and compares the parameters between simulated and measured values. The paper is organized in three major sections, antenna design, result analysis and finally concluding remarks respectively.

2. ANTENNAS DESIGN AND FORMULATION

2.1. Theoretical Modelling

The design formulation of microstrip antenna model is described in three sections as follows:

(i) The full wave approach is considered for antenna modelling, and the method of moments as a numerical technique is applied. Their steps of analysis are summarised in Figure 1.

Received 10 November 2017, Accepted 2 December 2017, Scheduled 16 January 2018
* Corresponding author: Prasanna Kumar Singh (singhprasanna25@yahoo.com).
The authors are with the Department of Electronics and Communication Engineering, Jaypee Institute of Information Technology, A10, Sector-62, Noida, Uttar Pradesh 201307, India.

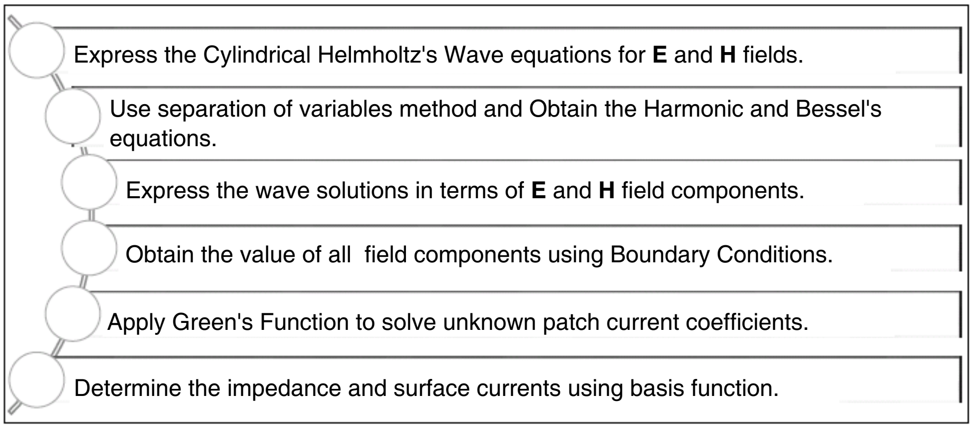

Figure 1. Steps of analysis for numerical technique.

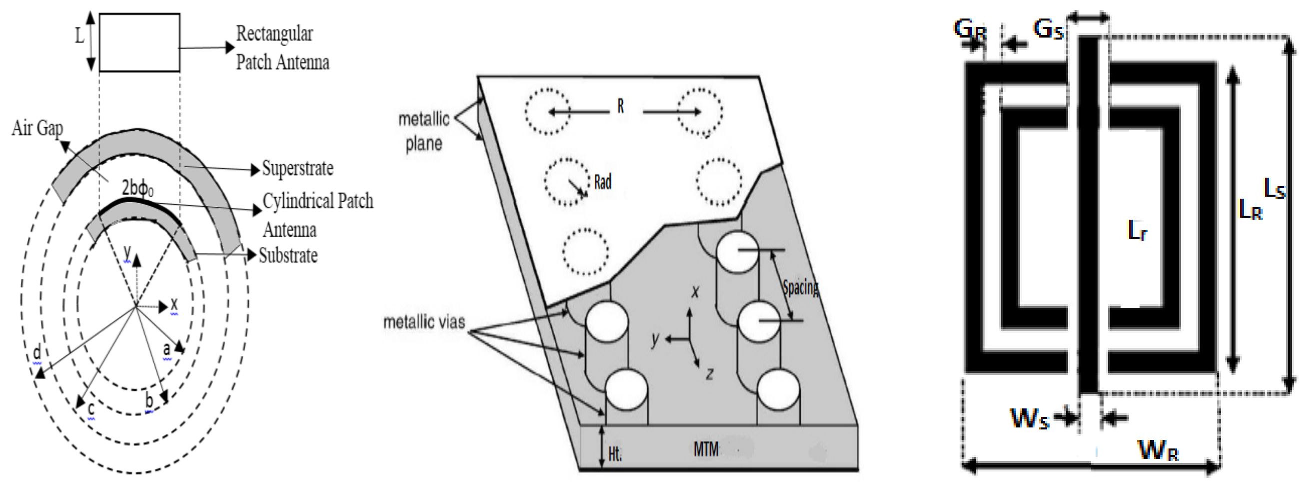

(a) (b) (c)

Figure 2. (a) Cylindrical-rectangular microstrip antenna with superstrate gap. (b) SIW with cylindrical metallize vias. (c) MTM using split rectangular ring resonator with metallic wire strip.

Assume a cylindrical ground and antenna surface as a perfect electrical conductor with superstrate air gap. Each antenna is excited separately by circumferential microstrip inset feeding with perfect impedance match and takes up to be line source with a unit amplitude density. The antenna model is assumed infinite and homogeneous in the ϕ and z-planes. The z components of the electric and magnetic fields in the ith region are varied from inner cylindrical core to free air as shown in Figure 2(a) and can be expressed in terms of functions in a cylindrical coordinate system:

$$E_{iz}(\rho,\,\phi,\,z) = \frac{1}{2\pi}\sum_{n=-\infty}^{\infty} e^{jn\phi}\int_{-\infty}^{\infty} dk_z\, e^{-jk_z z}\left[A_{in}H_n^{(2)}(k_{i\rho}\rho) + B_{in}\,J_n(k_{i\rho}\rho)\right] \tag{1}$$

$$H_{iz}(\rho,\,\phi,\,z) = \frac{1}{2\pi}\sum_{n=-\infty}^{\infty} e^{jn\phi}\int_{-\infty}^{\infty} dk_z\, e^{-jk_z z}\left[C_{in}H_n^{(2)}(k_{i\rho}\rho) + D_{in}\,J_n(k_{i\rho}\rho)\right] \tag{2}$$

where k_z is the propagation constant, $k_{i\rho}^2 = \omega^2\mu_0\varepsilon_i - k_z^2$, $\varepsilon_i = \varepsilon_0\varepsilon_{ri}$, and A_{in}, B_{in}, C_{in}, D_{in} are the unknown expansion coefficients of harmonic order n and functions k_z. $H_n^{(2)}(x)$, $J_n(x)$ are, respectively, the Hankel function of the second kind and Bessel function, of order n and argument

x. The transverse field components in the ith region can be obtained from E_{iz} and H_{iz}. Using the exact Green's function approach and applying boundary conditions, the far zone field components and other parameter can be determined [1, 4, 6].

(ii) The split rectangular ring resonator (SRRR) and strip wire on either side of the substrate for achieving MTM and placement of metallic vias for SIW technology are to be calculated and designed using standard design procedures [14, 17, 19]. The given SIW equation ensures the minimum leakage losses between via holes [18]:

$$\frac{\text{Spacing}}{2\text{Rad}} < 2 \quad \text{and} \quad \frac{2\text{Rad}}{R} < 0.2 \tag{3}$$

where, Rad and spacing are the radius and spacing of the consecutive metallized via holes, respectively, and R is the distance between two opposite rows of metallized vias of the SIW as shown in Figure 2(b). The propagation in SIW can only perform TE_{m0} modes of traditional rectangular waveguide, in which the E-field is perpendicular to the direction of propagation. It is found that the following requirements can be put forward to minimize return and leakage losses, that is, the diameter of hole should satisfy some geometric constraints [19]:

$$2\text{Rad} < \frac{\lambda_g}{5} \quad \text{and} \quad \text{Spacing} \leq 4\text{Rad} \tag{4}$$

(iii) The MTM unit cell employs SRRR and strip wire as shown in Figure 2(c). Thin strip wire structures produce effective negative dielectric permittivity below the plasma frequency, and the SRRR can result in an effective negative permeability over a particular frequency range. The optimum position of strip wire should be just behind the gap in SRRR, on the opposite side of the substrate. This position gives a robust Left Handed transmission, because of the fields generated due to interaction between SRRR and strip wire. Also, there is a little overlap between their magnetic fields, so the behavior of each component is not significantly affected by the presence of the other. On the other hand, if the thickness of substrate is reduced, it will enhance the strength of total resonance, increasing the value of negative permittivity as well as negative permeability [20, 21]. By controlling these two structures the effective permittivity and permeability can be changed separately, giving the capability to control the position of double negative regime.

The particulars of the antenna model are presented in Table 1.

Table 1. Specifications of antenna model (in mm).

Patch Antenna	Patch Length	Patch Width	Substrate Length	Substrate Width	Feeding Length	Feeding Depth	Inset Gap
	28.52	33.86	52.52	47.86	24.8	6	7.5
MTM Unit Cell	L_s	W_s	L_R	W_R	G_s	G_R	L_r
	38	1	32.58	41.92	2	1.5	30.08
SIW	Via Rad	Via Spacing	Via Row, R	Via Height, H_t			
	0.6	2.5	31.2	0.127			

2.2. Model Description

With the help of calculated data as tabulated in Table 1, the cylindrically mounted hybrid single and dual patch antennas using MTM with SIW are drawn in HFSS as shown in Figure 3. The present design analysis is usable for RT Duroid 5880 as MTM structure with small thickness of 5 mils. This MTM makes the antenna work on double negative medium of permittivity and permeability. With the proper use of SIW and MTM, this hybrid patch antenna satisfies the technical requirement on the flexible varying cylindrical surface. The split ring and strip wire form MTM for substrate and superstrate with same thickness [14, 15]. The MTM superstrate located at quarter wavelength forms partial reflective left handed material which not only acts as a protective shield but also controls the key parameters [4, 5, 16, 17].

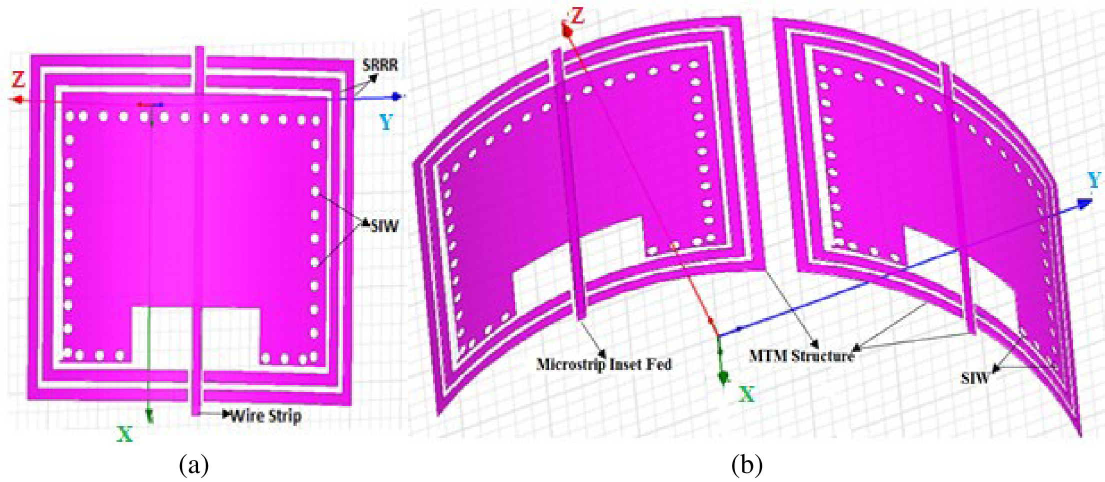

Figure 3. Geometry of rectangular hybrid antenna mounted on the cylindrical surface. (a) Single antenna model. (b) Dual antenna model.

The microstrip inset feed is used for exciting the antenna model and adjusted at 50 ohm impedance matching. The combination of these arrangements makes the antenna configurations work as a cavity resonator. Initially, the dimension specifications of single and dual antenna models are calculated and validated on the planar surface [4, 5]. Both antenna models are transformed step by step from planar surface to cylindrical surface, and the corresponding parametric variations at different diameters are noted down. For dual patch antenna, the mutual coupling is an important concern which depends on the inter element spacing and angle of mounting curvature. In this case, the H-plane antenna is considered with fixed inter element spacing at half wavelength for maximum radiation. The SIW technology effectively controls the surface waves and hence minimizes the mutual coupling effect for dense antenna array design.

Table 2. Comparative parametric study of single hybrid antenna on varying diameter.

Cylindrical Diameter (mm)	Simulated Results			Measured Results		
	Resonant Freq. (GHz)	Gain (dB)	% Bandwidth	Resonant Freq. (GHz)	Gain (dB)	% Bandwidth
100	5.3	7.7	6.8	4.9	6.9	5.1
500	4.7	8.5	7.1	4.4	7.4	6.3
1000	4.5	9.2	8.4	4.2	8.3	7.8

Table 3. Comparative parametric study of dual hybrid antenna on varying diameter.

Cylindrical Diameter (mm)	Simulated Results			Measured Results		
	Resonant Freq. (GHz)	Gain (dB)	% Bandwidth	Resonant Freq. (GHz)	Gain (dB)	% Bandwidth
100	5.9	9.5	12.8	5.2	8.6	11.5
500	5.4	10.3	13.4	4.9	9.8	12.7
1000	5	12.1	15.6	4.4	10.9	14.3

3. RESULT ANALYSIS

The simulated and experimental results of single and dual antenna models are obtained and tabulated in Tables 2 and 3. The variations in resonant frequency are due to change in dielectric property at various diameters and maintain the overall performances with the adoption of hybrid combination. The operating frequency deviates smoothly over the C-band with diameter limit from 100 mm to 1000 mm for both antenna models. Beyond this lower bending diameter, the dielectric material cracks, and the structure shows an abnormal behaviour. Also, the bending movement should be very gradually and carefully in order to avoid any damage. Even though the elements are placed very close to each other, the

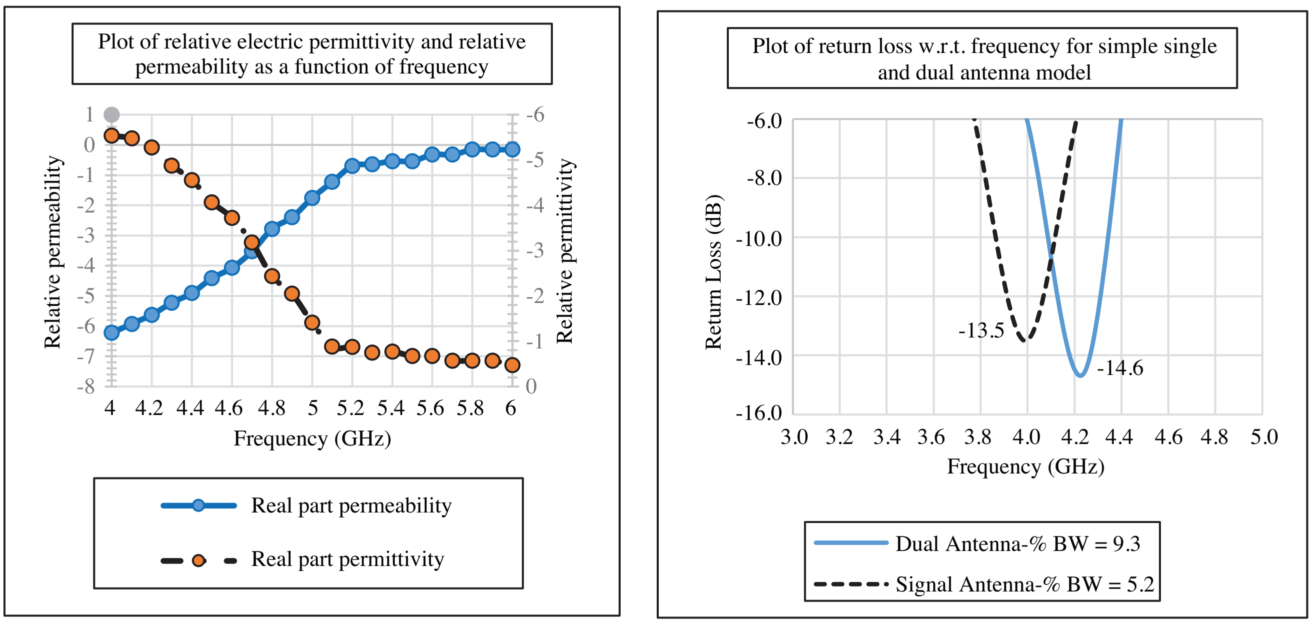

(a) (b)

Figure 4. (a) MTM structure behaviour in terms of epsilon-negative and mu-negative. (b) Performance of simple antenna model in terms of percentage bandwidth.

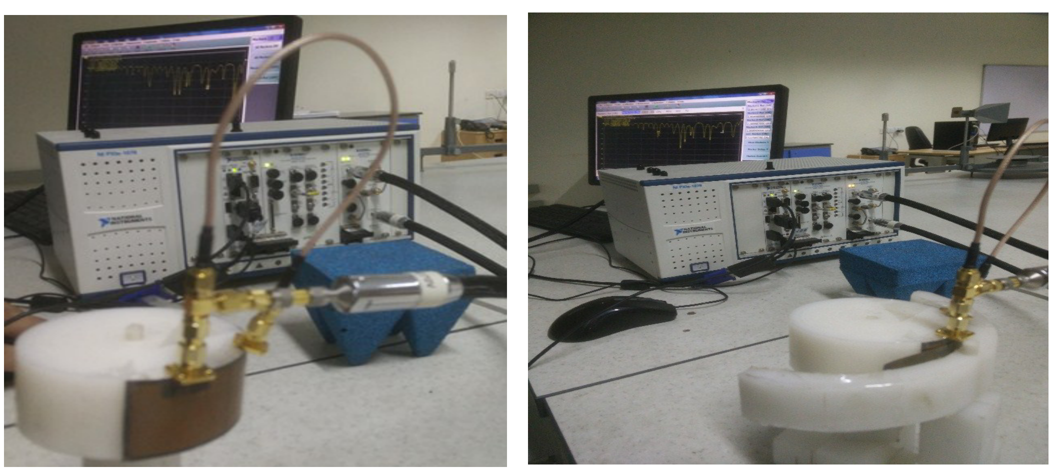

(a) (b)

Figure 5. Experiment set up for the dual antenna model on the cylindrical surface, (a) without superstrate, (b) with superstrate.

results of dual antenna model is better due to the shielding effects of SIW and MTM. The behaviour of the MTM structure is also drawn in Figure 4(a) in terms of negative permittivity and negative permeability as a function of frequency. Also, in Figure 4(b), the 9.3% and 5.2% bandwidth performances of simple antenna models (without integration of MTM and SIW) are depicted for single and dual antennas, respectively. The laboratory set up for measuring the fabricated antenna performance is shown in Figure 5. Figures 6 and 7 show the plot of bandwidth and gain for the antenna models at a significant diameter of 1000 mm. The simulated result shows 9.2 dB and 12.1 dB gains with bandwidths of 8.4% and 15.6% of single and dual antenna models, respectively. The obtained results of hybrid antenna models are better and improved as compared to the simple antenna model's performance. The

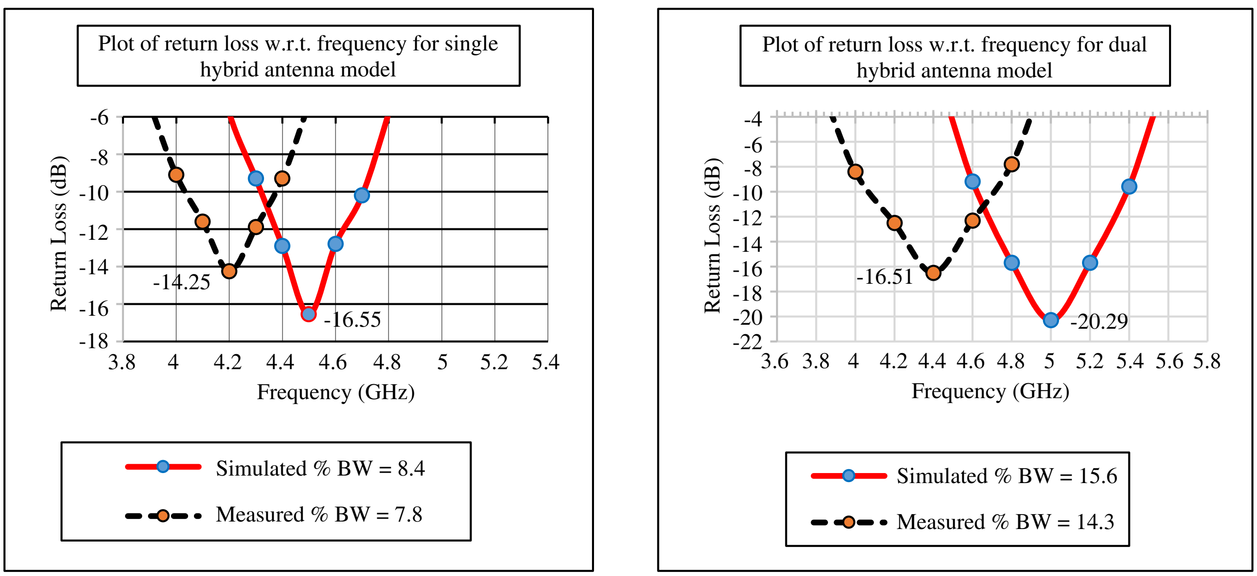

(a) (b)

Figure 6. Bandwidth comparison plot between simulated and measured values of hybrid antenna mounted on the cylindrical diameter at 1000 mm surface. (a) Single antenna. (b) Dual antenna.

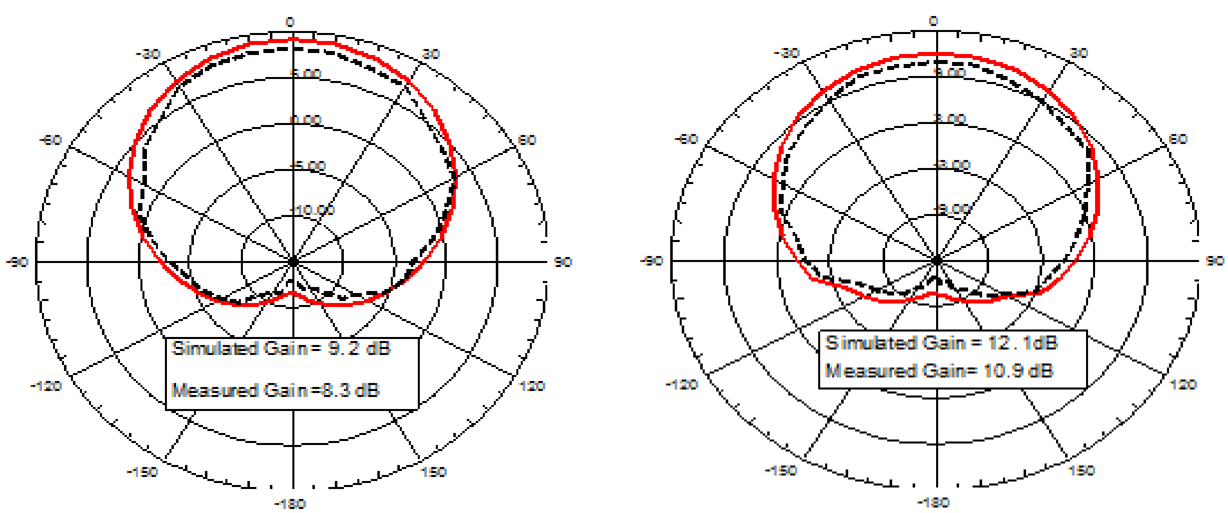

(a) (b)

Figure 7. Gain comparison plot between simulated and measured values of hybrid antenna mounted on the cylindrical surface at 1000 mm diameter. (a) Single antenna. (b) Dual antenna.

experimental results are in good agreement with simulated values, and hence, the given antenna models are recommended as reconfigurable antennas. The microstrip reconfigurable antennas have great calibre to work on varying non-planar platform with multiple wireless standards.

4. CONCLUSIONS AND FUTURE WORK

It is observed that the proposed hybrid microstrip antenna model not only executes as frequency reconfigurable but also provides the better gain and wide bandwidth. Also, the suggested reconfigurable antenna model works on a simple mechanism with improved performance which is a distinctive in its category. The presented antenna model will be more practical in several non-planar commercial and military applications. The novel MTM and SIW integration further strengthens its competency and inspires the new scope.

REFERENCES

1. Wong, K.-L., *Design of Nonplanar Microstrip Antennas and Transmission Lines*, 16–30, John Wiley & Sons Inc., New York, 1999.
2. Josefsson, L. and P. Persson, *Conformal Array Antenna Theory and Design*, 155–258, John Wiley & Sons Inc., New Jersey, 2006.
3. Tam, W. Y., A. K. Y. Lai, and K. M. Luk, "Mutual coupling between cylindrical rectangular microstrip antennas," *IEEE Transactions on Antennas and Propagation*, Vol. 43, No. 8, 897–899, August 1995.
4. Singh, P. K. and J. Saini, "Effect of varying curvature and inter element spacing on dielectric coated conformal microstrip antenna array," *Progress In Electromagnetics Research M*, Vol. 58, 11–19, 2017.
5. Singh, P. K. and J. Saini, "Performance analysis of superstrate loaded cylindrically conformal microstrip antenna on the varying curvature for WiMAX applications," *International Journal of Microwave and Optical Technology*, Vol. 11, No. 6, 406–412, November 2016.
6. Cooray, F. R., and J. S. Kot, "Analysis of radiation from a cylindrical-rectangular microstrip patch antenna loaded with a superstrate and an air gap, using the electric surface current model," *Progress In Electromagnetics Research*, Vol. 67, 135–152, 2007.
7. Majid, H. A., M. K. Abd Rahim, and T. Masri, "Microstrip antenna's gain enhancement using left-handed metamaterial structure," *Progress In Electromagnetics Research M*, Vol. 8, 235–247, 2009.
8. Mahmoud, S. F., "A new miniaturized annular ring patch resonator partially loaded by a metamaterial ring with negative permeability and permittivity," *IEEE Antennas and Wireless Propagation Letters*, Vol. 3, 19–22, April 2004.
9. Wang, H., D.-G. Fang, B. Zhang, and W.-Q. Che, "Dielectric loaded substrate integrated waveguide (SIW) H-plane horn antennas," *IEEE Transactions on Antennas and Propagation*, Vol. 58, No. 3, 640–647, March 2010.
10. Caytan, O., S. Lemey, S. Agneessens, and H. Rogier, "SIW antennas as hybrid energy harvesting and power management platforms for the internet of things," *International Journal of Microwave and Wireless Technologies*, 1–9, 2016.
11. Luo, G. Q., Z. F. Hu, W. J. Li, X. H. Zhang, L. L. Sun, and J. F. Zheng, "Bandwidth-enhanced low-profile cavity-backed slot antenna by using hybrid SIW cavity modes," *IEEE Transactions on Antennas and Propagation*, Vol. 60, No. 4, 1698–1704, 2012.
12. Luo, G. Q., T. Y. Wang, and X. H. Zhang, "Review of low profile substrate integrated waveguide cavity backed antennas," *International Journal of Antennas and Propagation*, 1–7, Hindawi Publishing Corporation, 2013.
13. Jim'enez-Fern'andez, M. J., R. Torres-S'anchez, and P. Otero, "Cavity-backed slot array antenna in substrate-integrated waveguide technology," *Microwave and Optical Technology Letters*, Vol. 53, No. 9, 2105–2108, 2011.

14. Pendry, J. B., A. J. Holden, D. J. Robbins, and W. J. Stewart, "Magnetism from conductors and enhanced nonlinear phenomena," *IEEE Transactions on Microwave Theory and Tech.*, Vol. 47, No. 11, 2075–2084, November 1999.
15. Capolino, F., *Handbook of Artificial Materials: Applications of Metamaterials*, Vol. 2, 18.1–18.14, Taylor and Francis, CRC Press, October 2009.
16. Deslandes, D. and K. Wu, "Single-substrate integration technique of planar circuits and waveguide components," *IEEE Transactions on Microwave Theory and Tech.*, Vol. 51, 593–596, 2003.
17. Meagher, C. J. and S. K. Sharma, "A wideband aperture-coupled microstrip patch antenna employing spaced dielectric cover for enhanced gain performance," *IEEE Transactions on Antennas and Propagation*, Vol. 58, No. 9, 314–318, September 1982.
18. Yang, H. Y. and N. G. Alexopoulos, "Gain enhancement methods for printed circuit antennas through multiple superstrates," *IEEE Transactions on Antennas and Propagation*, Vol. 35, No. 8, 860–863, July 1987.
19. Djerafi, T., A. Doghri, and K. Wu, "Substrate integrated waveguide antennas," *Handbook of Antenna Technologies, Springer Science + Business Media Singapore*, 1–60, 2015.
20. Cui, T. J., D. Smith, and R. Liu, *Metamaterials: Theory, Design, and Applications*, Springer, Berlin, Germany, 2009.
21. Engheta, N. and R. W. Ziolkowski, *Metamaterial Physics* & *Engineering Explorations*, Wiley-IEEE Press, June 2006.